A significant impact of nitrogen substitution on the solid state electronic structure: a case of 1,3,6,8-tetrakis(methylchalcogeno)-2,7-diazapyrene

Krill Bulgarevich,[a] Kazuo Takimiya,[a,b,c*]

[a] RIKEN Center for Emergent Matter Science (CEMS), 2-1 Hirosawa, Wako, Saitama 351-0198, Japan

[b] Tohoku University Advanced Institute for Materials Research (AIMR), 2-1-1 Katahira, Aoba-ku, Sendai, Miyagi 980-8577 Japan

[c] Department of Chemistry, Graduate School of Science, Tohoku University, 6-3 Aoba, Aramaki, Aoba-ku, Sendai, Miyagi 980-8578 Japan

Contents

1. MO-azapyrene-based single-crystal transistor

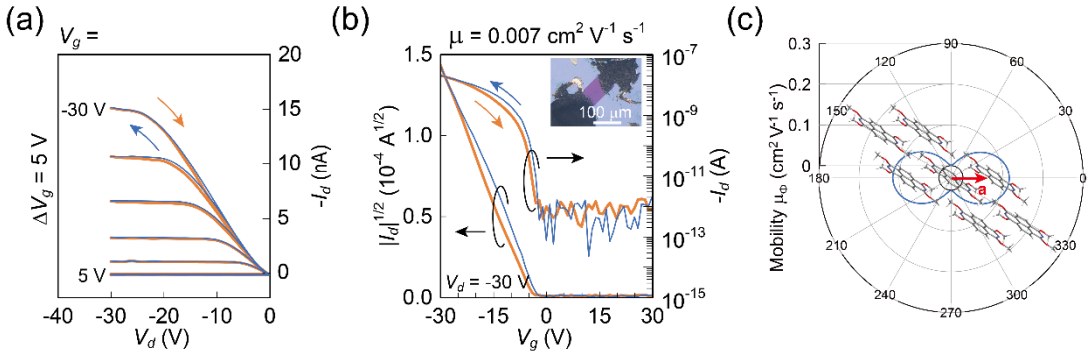

Fig. S1. (a) Output and (b) transfer characteristics of MO-azapyrene, and (c) simulated anisotropic mobility based on the hopping model.

2. Attempted synthesis of 1,3,6,8-tetrakis(methylthio)-2,7-diazapyrene from 1a

A dry flask was charged with 1,3,6,8-tetra(pivaloxy)-2,7-diazapyrene (**1a**)[1, 2] (0.05 g, 0.08 mmol) and dry *N,N*-dimethylformamide (DMF, 30 mL). Methyl 3-(methylthio)propionate (0.10 mL, 0.8 mmol) and potassium tert-butoxide (tBuOK, 0.15 g, 1.3 mmol) were added under a flow of nitrogen. The reaction mixture was stirred at 100 °C for 16 h. After cooling to room temperature, the mixture was poured into water (ca. 50 mL) and filtered. The formation of 1,3,6,8-tetrakis(methylthio)-2,7-diazapyrene was not confirmed by APCI mass spectroscopy.

A dry flask was charged with **1a** (0.05 g, 0.08 mmol) and tetrakis(triphenylphosphine)palladium(0) ($Pd[PPh_3]_4$, 0.02 g, 0.017 mmol). Dry toluene (30 mL) and tributyl(methylthio)stannane ($MeS\text{-}SnBu_3$, 0.20 mL, 0.7 mmol) were added under a nitrogen atmosphere, and the reaction mixture was stirred at 120 °C for 16 h. After cooling to room temperature, the mixture was poured into methanol and filtered. The formation of 1,3,6,8-tetrakis(methylthio)-2,7-diazapyrene was not confirmed by APCI mass spectroscopy; a weak signal consistent with a mono-substituted product (1,3,6-tris(pivaloxy)-8-methylthio-2,7-diazapyrene) was observed.

3. Crystallographic data

Table S1. Crystallographic parameters of MT-azapyrene.

Compound	MT-azapyrene	MT-azapyrene	MT-azapyrene
Temperature / K	300	200	100
Formula	$C_{18}H_{16}N_2S_4$	$C_{18}H_{16}N_2S_4$	$C_{18}H_{16}N_2S_4$
Molecular Weight	388.580	388.580	388.580
Crystal Habit	plate	plate	plate
Crystal System	*triclinic*	*triclinic*	*triclinic*
Space Group	*P*-1	*P*-1	*P*-1
a /Å	5.28031(8)	5.24990(10)	5.22870(10)
b /Å	10.53118(15)	10.4549(2)	10.4035(2)
c /Å	15.2990(2)	15.2984(3)	15.2739(3)
α /°	91.9773(12)	93.4100(10)	93.978(2)
β /°	90.4976(13)	90.930(2)	91.140(2)
γ /°	94.2773(12)	93.8400(10)	93.599(2)
V /Å^3	847.81(2)	836.15(3)	826.97(3)
Z	2	2	2
R	0.0432	0.0382	0.0482
R_w	0.1266	0.1088	0.1478
GOF	1.073	1.064	0.971
CCDC	2528773	2528774	2528775

Table S2. Crystallographic parameters of MS-azapyrene.

Compound	MS-azapyrene	MS-azapyrene	MS-azapyrene
Temperature / K	300	200	100
Formula	$C_{18}H_{16}N_2Se_4$	$C_{18}H_{16}N_2Se_4$	$C_{18}H_{16}N_2Se_4$
Molecular Weight	576.224	576.224	576.224
Crystal Habit	needle	needle	needle
Crystal System	*triclinic*	*triclinic*	*triclinic*
Space Group	*P*-1	*P*-1	*P*-1
a /Å	5.3990(2)	5.3724(2)	5.3527(2)
b /Å	10.6215(4)	10.5552(4)	10.5040(2)
c /Å	15.7507(4)	15.7113(3)	15.6600(2)
α /°	95.774(3)	96.178(2)	96.335(2)
β /°	91.532(3)	91.672(2)	91.735(2)
γ /°	93.914(3)	93.573(3)	93.212(2)
V /Å^3	896.04(5)	883.46(5)	873.14(4)
Z	2	2	2
R	0.0482	0.0481	0.0463
R_w	0.1387	0.1427	0.1334
GOF	1.070	1.059	1.171
CCDC	2528776	2528777	2528778

Table S3. Crystallographic parameters of **2-5** and **1c**.

Compound	**2**	**3**	**4**	**5**	**1c**
Temperature / K	100	100	100	100	100
Formula	$C_7H_6BrCl_2N$	$C_{14}H_{10}Cl_4N_2$	$C_{14}H_8Cl_4N_2$	$C_{14}H_6Br_2Cl_4N_2$	$C_{14}H_4Cl_4N_2$
Molecular Weight	254.936	348.048	346.032	503.824	342.000
Crystal Habit	block	plate	plate	block	needle
Crystal System	*monoclinic*	*triclinic*	*monoclinic*	*triclinic*	*triclinic*
Space Group	$P2_1/n$	P-1	$P2_1/c$	P-1	P-1
a /Å	10.5727(2)	3.8934(3)	9.3169(5)	9.7620(3)	3.7607(2)
b /Å	7.19410(10)	6.3538(3)	22.5715(8)	12.4337(4)	12.1745(5)
c /Å	12.6552(2)	14.2061(8)	6.9712(3)	20.1351(5)	13.3853(6)
α /°	90	92.601(4)	90	78.679(2)	95.130(4)
β /°	112.668(2)	92.457(5)	111.748(6)	79.088(2)	92.479(4)
γ /°	90	90.210(4)	90	85.072(2)	97.667(4)
V /Å^3	888.21(3)	350.74(4)	1361.66(12)	2350.06(12)	603.984
Z	4	1	4	6	2
R	0.0311	0.0987	0.0712	0.0589	0.0854
R_w	0.0908	0.2858	0.2009	0.1414	0.2232
GOF	1.091	1.085	1.097	1.033	1.122
CCDC	2528768	2528769	2528770	2528771	2528772

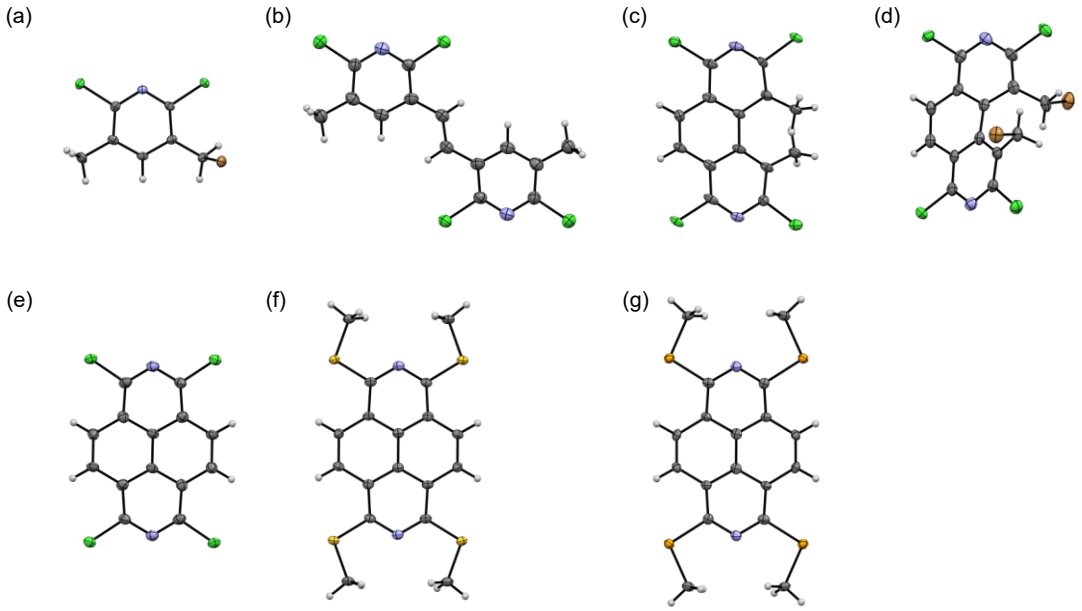

Fig. S2. Molecular structures of (a) **2**, (b) **3**, (c) **4**, (d) **5**, (e) **1c**, (f) MT-azapyrene, and (g) MS-azapyrene, determined by single-crystal XRD.

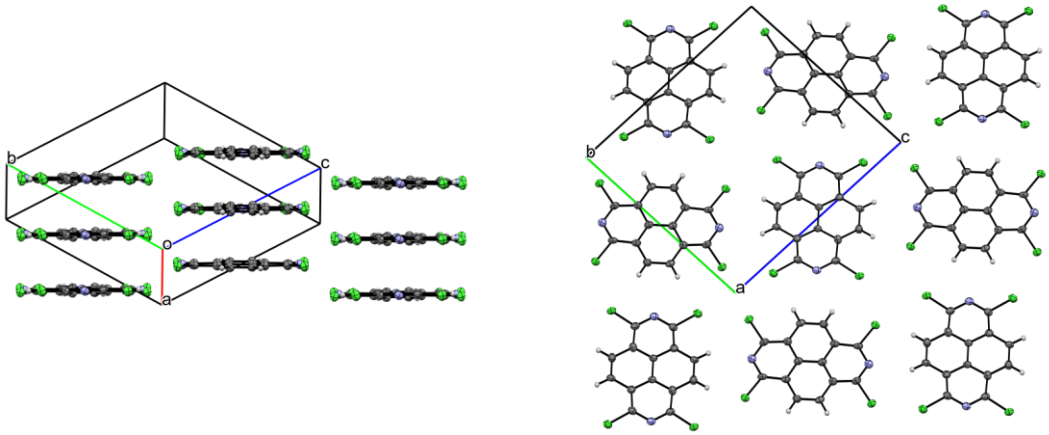

Fig. S3. Side (left) and top (right) view of the crystal structure of **1c**.

4. Physicochemical characterization

The molecular properties were evaluated by photoemission yield spectroscopy in air (Fig. S4), and UV-vis absorption spectra (Fig. S5), together with DFT calculations (Fig. S6). Due to the low solubility of the MX-azapyrenes, their HOMO energy levels were estimated from ionization potentials measured in the crystalline state. The optical band gaps (*E*g) were estimated from the absorption onset energies.

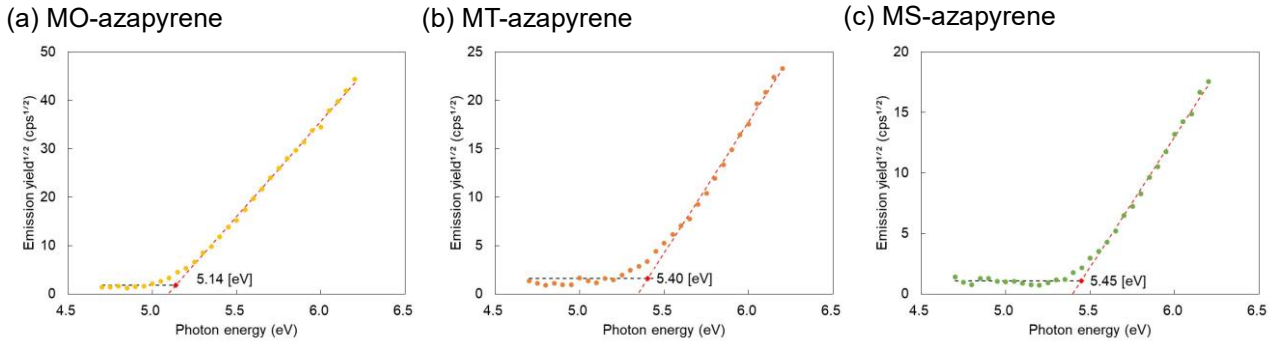

Fig. S4. Ionization potentials of (a) MO-, (b) MT, and (c) MS-azapyrene measured in air on a RIKEN-Keiki AC-2 system.

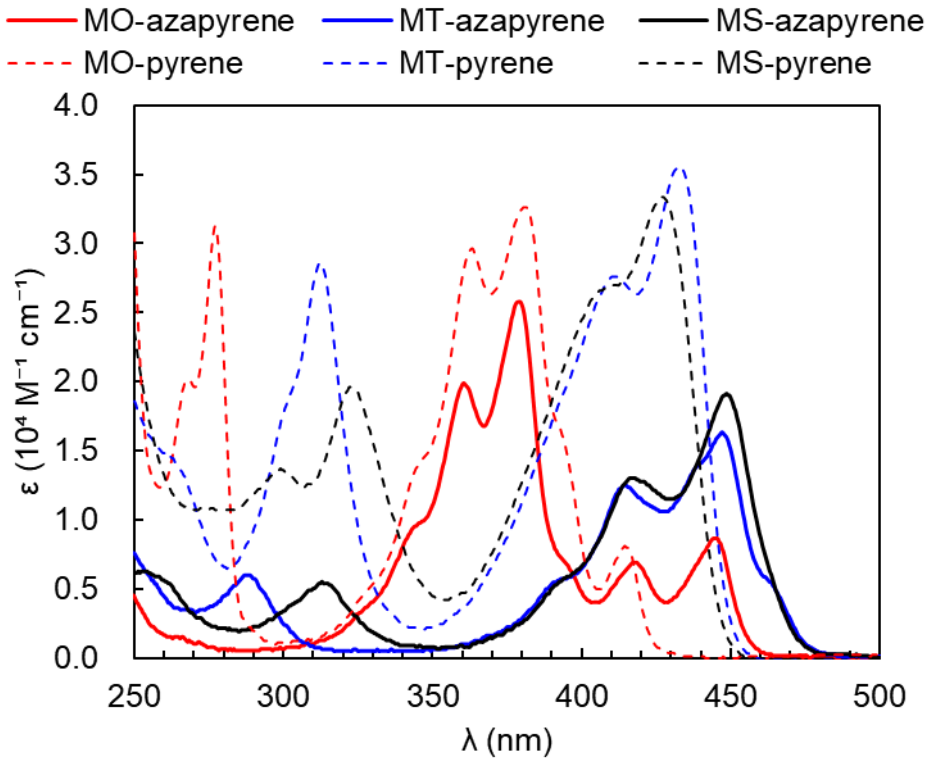

Fig. S5. UV-vis absorption spectra of MO-, MT-, and MS-azapyrene (solid lines) and MO-, MT-, MS-pyrene (dashed lines) in dichloromethane.

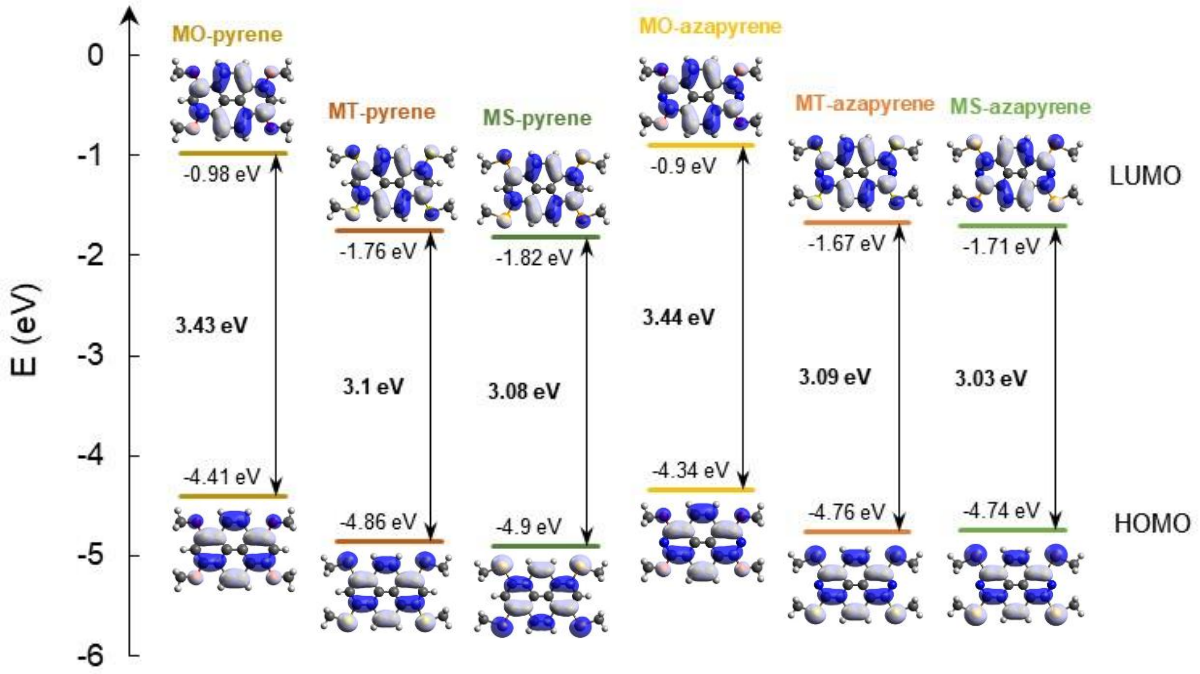

Fig. S6. Comparison of energy levels and frontier orbitals (HOMO and LUMO) for MO-, MT-, and MS-pyrenes and azapyrenes, calculated by the DFT methods at B3LYP/6-311G(d,p) level.

Table S4. Molecular electronic properties of MO-, MT-, and MS-azapyrene.

	IP (eV)[a]	λ_{max} (nm) / ε (×10^4)	λ_{onset} (nm) / E_g (eV)[b]	E_{HOMO}/ E_{LUMO} (eV)[c]
MO-azapyrene	5.14	445 / 0.86	457 / 2.71	–4.34/–0.90
MT-azapyrene	5.40	446 / 1.63	476 / 2.61	–4.76/–1.67
MS-azapyrene	5.45	449 / 1.91	474 / 2.62	–4.74/–1.71

[a] Determined from the onset potential in photoemission yield spectroscopy in air. [b] Optical bandgap determined from the onset of absorption spectra. [c] Obtained from theoretical calculations by the DFT method.

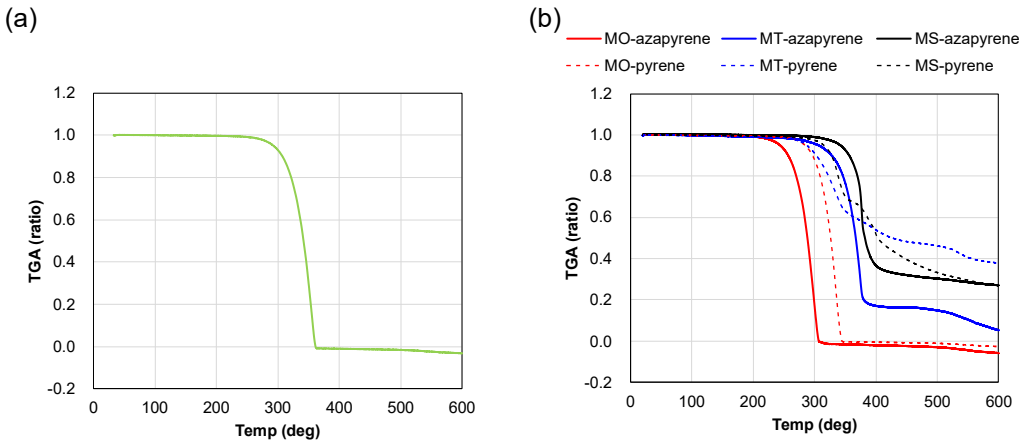

Fig. S7. Thermogravimetric analysis of (a) **1c** and (b) MO-, MT-, and MS-azapyrene (solid lines) and MO-, MT-, MS-pyrene (dashed lines), measured in nitrogen at a heating rate of 5 °C min^{-1}.

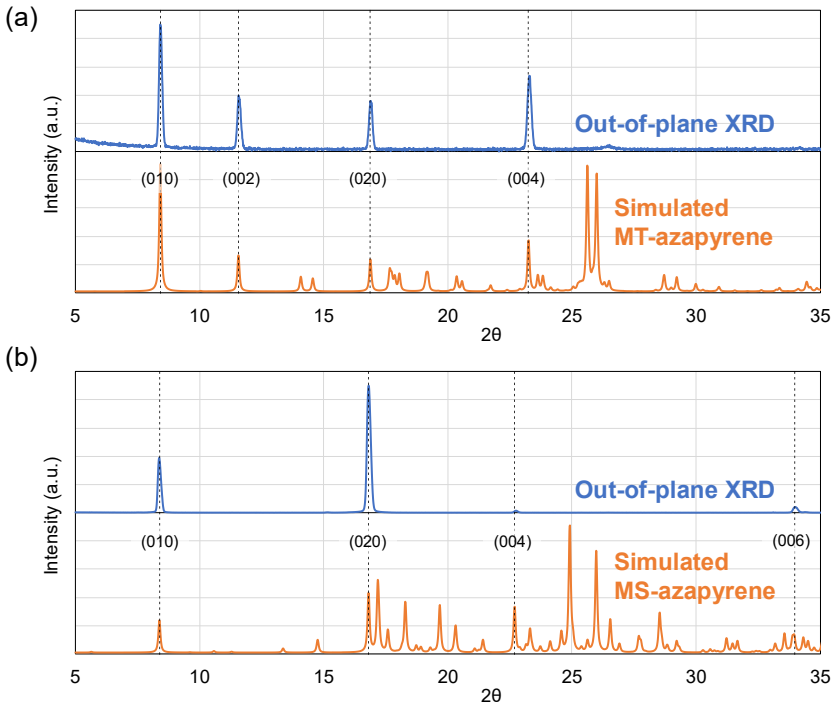

Fig. S8. Out-of-plane XRD of (a) MT- and (b) MS-azapyrene single-crystals transferred onto CYTOP / SiO_2 surface.

5. Characterization of charge transport

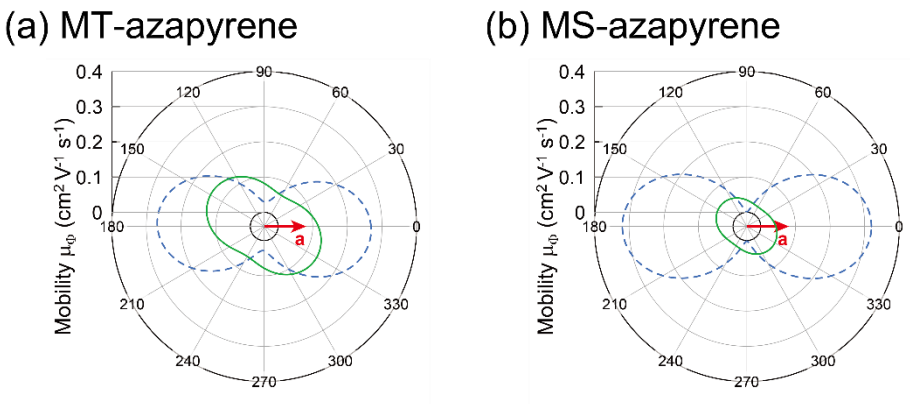

Fig. S9. Mobility orientation function calculated for MT- and MS-azapyrene using transfer integrals evaluated for two non-equivalent π-stacking layers (solid and dashed lines).

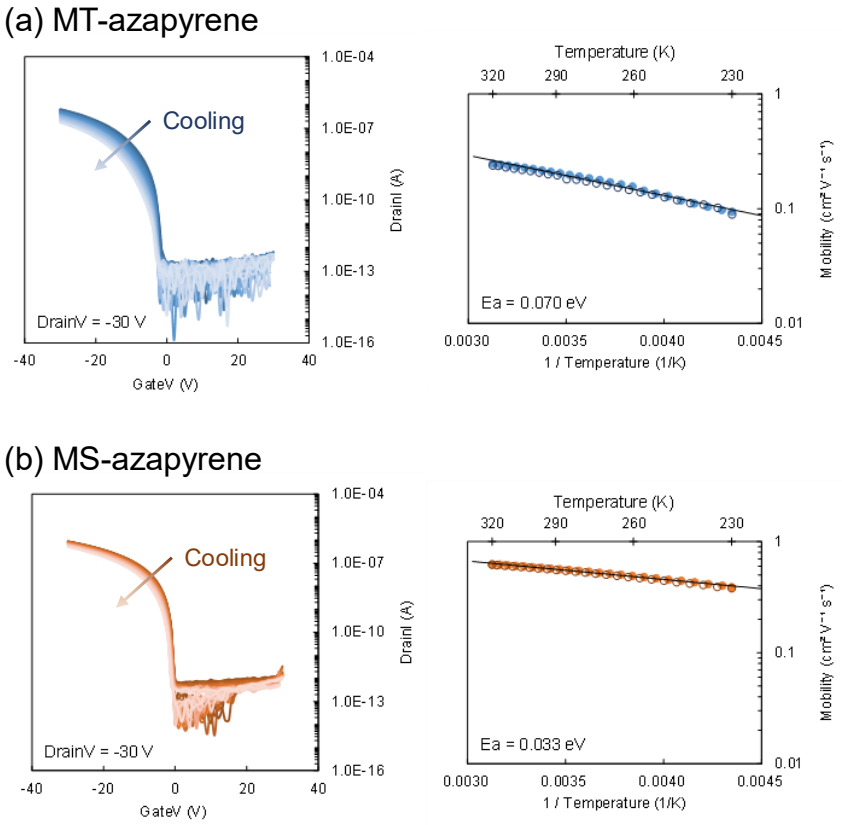

Fig. S10. Temperature dependence of transfer characteristics and carrier mobility of (a) MT- and (b) MS-azapyrene measured in vacuum (<1 Pa). Filled and open markers in the right figures represent mobilities extracted from the cooling and heating cycles, respectively. The estimated activation energy values are indicated.

6. Quadrupole moments calculated for MX-azapyrenes and MX-pyrenes

Table S5. Quadrupole moments[3] calculated for MX-azapyrenes and MX-pyrenes using the Gaussian16 program at B3LYP/6-31G(d,p) level. The molecules were placed at the origin of the xy-plane so that their long axes were aligned with the *x*-axis.

Compound	Q_{xx}	Q_{yy}	Q_{zz}	Q_{yy}/Q_{xx}
MO-azapyrene	37.29	-13.91	-23.39	-0.373
MT-azapyrene	43.67	-19.01	-24.66	-0.435
MS-azapyrene	41.77	-16.01	-25.76	-0.383
MO-pyrene	24.55	-8.53	-16.02	-0.347
MT-pyrene	29.31	-12.23	-17.09	-0.417
MS-pyrene	28.16	-9.80	-18.36	-0.348

7. NMR spectra

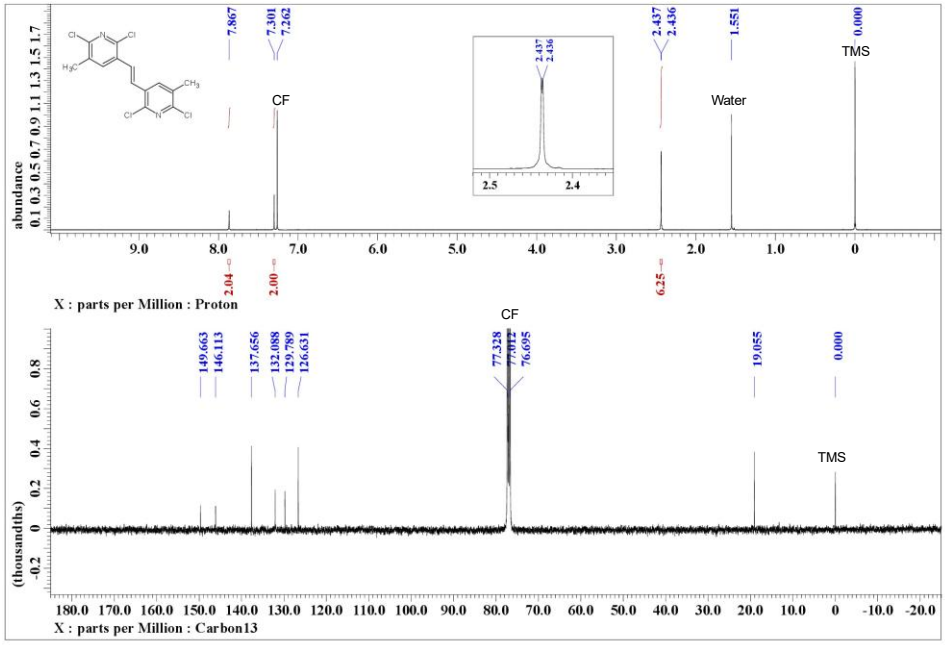

Fig. S11. ^{1}H (top) and ^{13}C (bottom) NMR spectra of 1,2-bis(2,6-dichloro-5-methylpyridin-3-yl)ethene (**3**) in $CDCl_3$.

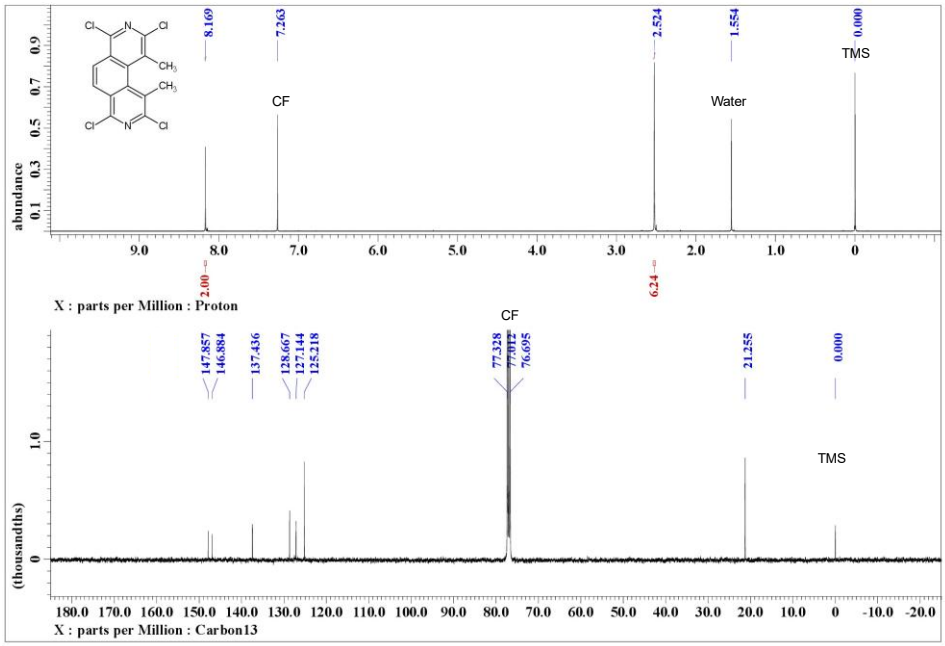

Fig. S12. ^{1}H (top) and ^{13}C (bottom) NMR spectra of 2,4,7,9-tetrachloro-1,10-dimethyl-3,8-phenanthroline (**4**) in $CDCl_3$.

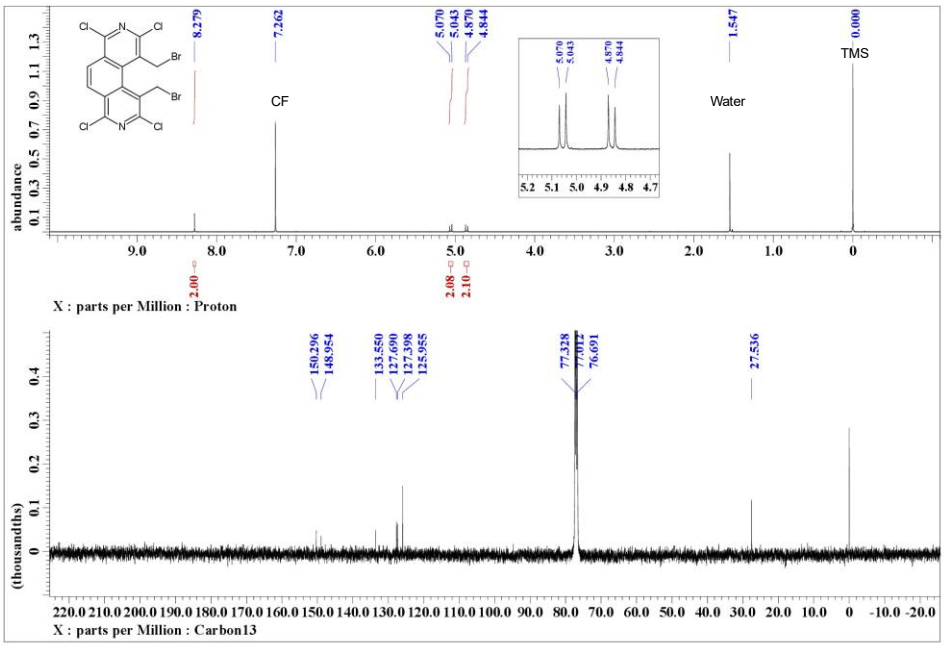

Fig. S13. ^{1}H (top) and ^{13}C (bottom) NMR spectra of 1,10-bis(bromomethyl)-2,4,7,9-tetrachloro-3,8-phenanthroline (**5**) in $CDCl_3$.

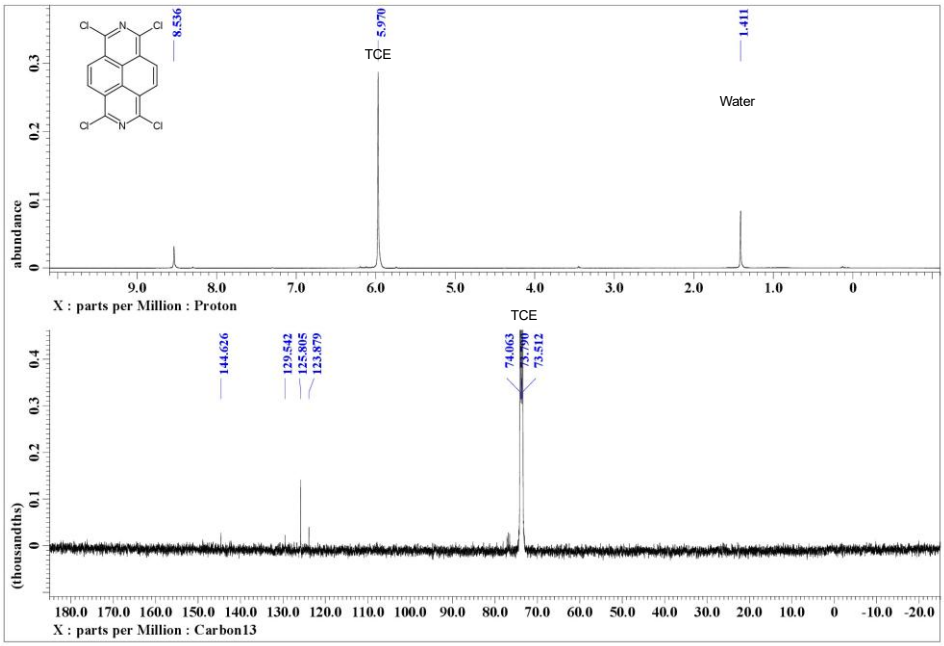

Fig. S14. ^{1}H (top) and ^{13}C (bottom) NMR spectra of 1,3,6,8-tetrachloro-2,7-diazapyrene (**1c**) in 1,1,2,2-tetrachloroethane-d_2 at 130 °C.

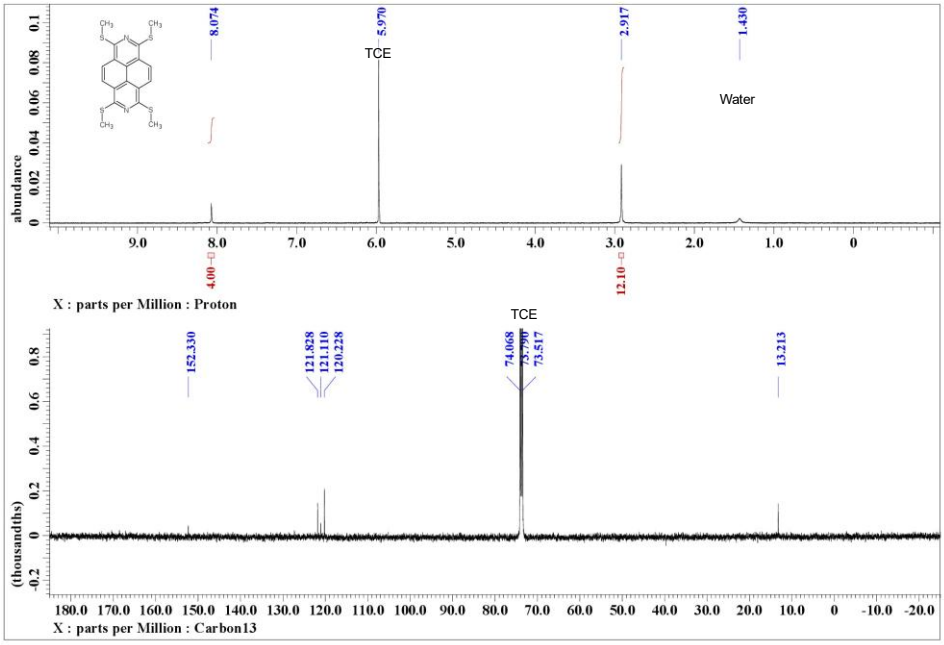

Fig. S15. ^{1}H (top) and ^{13}C (bottom) NMR spectra of 1,3,6,8-tetrakis(methylthio)-2,7-diazapyrene (MT-azapyrene) in 1,1,2,2-tetrachloroethane-d_2 at 120 °C.

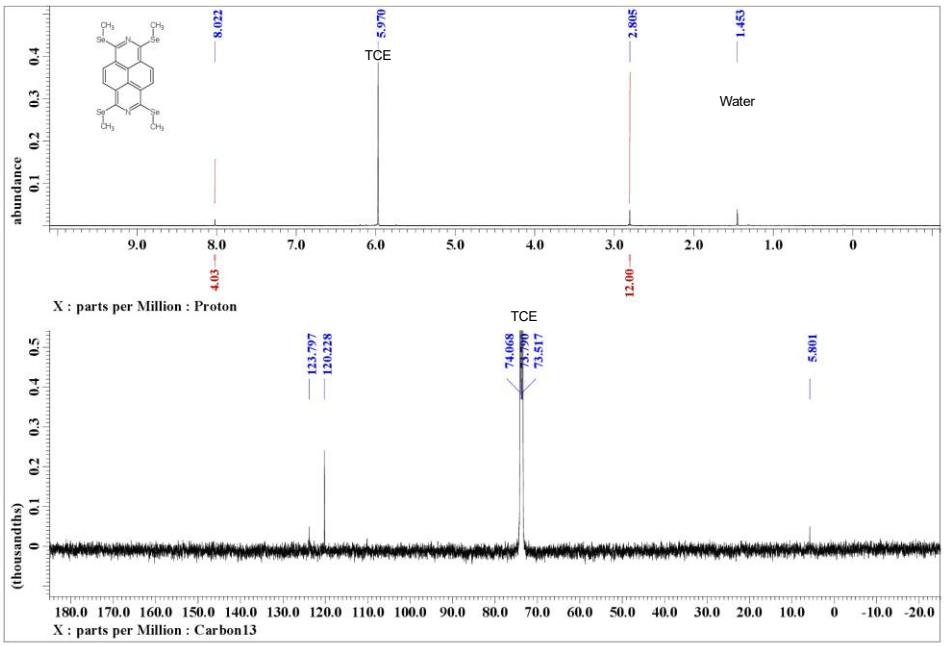

Fig. S16. ^{1}H (top, 100°C) and ^{13}C (bottom, 130 °C) NMR spectra of 1,3,6,8-tetrakis(methylseleno)-2,7-diazapyrene (MS-azapyrene) in 1,1,2,2-tetrachloroethane-d_2.

8. References

1. T. Nakazato, T. Kamatsuka, J. Inoue, T. Sakurai, S. Seki, H. Shinokubo and Y. Miyake, The reductive aromatization of naphthalene diimide: a versatile platform for 2,7-diazapyrenes, *Chem. Commun.*, 2018, **54**, 5177-5180.
2. T. Nakazato, W. Matsuda, T. Sakurai, S. Seki, H. Shinokubo and Y. Miyake, Synthesis and Crystal Packing Structures of 2,7-Diazapyrenes with Various Alkyl Groups at 1,3,6,8-Positions, *Chem. Lett.*, 2020, **49**, 465-468.
3. T. Mori, Quadrupole moments determine the crystal structures of organic semiconductors, *J. Mater. Chem. C*, 2025, **13**, 17078-17093.